ARTICLE IN PRESS

Available online at www.sciencedirect.com
ScienceDirect
Journal of Photochemistry and Photobiology B: Biology 90 (2008) 69–77
Journal of Photochemistry and Photobiology B:Biology
www.elsevier.com/locate/jphotobiol

Spectroscopic studies on the effect of temperature on pH-induced folded states of human serum albumin

Ajay Kumar Shaw, Samir Kumar Pal *

Unit for Nano Science and Technology, Department of Chemical, Biological and Macromolecular Sciences, S.N. Bose National Centre for Basic Sciences, Block JD, Sector III, Salt Lake, Kolkata 700 098, India

Received 28 July 2007; received in revised form 8 November 2007; accepted 12 November 2007

Abstract

Human serum albumin (HSA) is a very important multi-domain transporter protein in the circulatory system responsible for carriage of various kinds of ligands within the physiological system. HSA is also known to undergo conformational transformation at different pH(s) and temperatures. In this report we have studied the binding interactions of a photosensitizing drug, protoporphyrin IX (PPIX) with various conformers of HSA at different temperatures using picosecond time-resolved fluorescence spectroscopy. Also, using dynamic light scattering (DLS) and circular dichroism (CD) spectroscopy we have followed the structural transition of various conformers of HSA at different temperatures. Ensuring the intact binding of PPIX to various conformers of HSA at different temperatures as revealed through time-resolved fluorescence anisotropy decay and significant spectral overlap of emission of Trp214 residue (donor) in domain-IIA and absorption of PPIX (acceptor) bound to domain-IB of HSA, we have applied Förster's resonance energy transfer (FRET) technique to determine the interdomain separation under various environmental conditions. The alkali-induced conformer of HSA shows almost no change in donor–acceptor distance in contrast to the native and acid-induced conformers of HSA, which show a decrease in distance with increase in temperature. Through this study the non-covalently bound PPIX is shown to be an efficient FRET probe in reporting the different temperature-induced folded states of HSA in buffer solutions of widely differing pH values.

Keywords: Human serum albumin (HSA); FRET; Fluorescence anisotropy; PPIX–HSA complex; Thermal unfolding; Inter-domain separation

1. Introduction

Serum albumins are the most abundant proteins present in the circulatory system [1]. They act as carrier for many endogenous substances like fatty acids, bilirubins, hormones and numerous small ligands [2–5]. Human serum albumin (HSA) (molecular weight 66,479 Da) comprising of 585 amino acid residues is a heart-shaped tridomain protein with each domain subdivided into two identical subdomains A and B [6]. Its amino acid sequence comprises of 17 disulfide bridges distributed over all domains, one free thiol (Cys34) in domain-I and a tryptophan residue (Trp214) in domain-IIA. HSA binds a wide variety of ligands with principal binding site being present in domains-IIA and IIIA [4]. HSA acts as an endogenous carrier of photosensitizing drugs known as porphyrins [7]. Porphyrins belong to a class of tetrapyrroles having extensive applications as photosensitizers in medicine [8,9]. Porphyrins are spectroscopically well characterized [10–12] and are known to serve as models for artificial solar energy capture as in photosynthesis [13]. The interaction of porphyrins with serum albumins has been a subject of extensive research till date [14–18]. Crystallographic study [19] reveals that protoporphyrin IX (PPIX), a member of porphyrin family, binds to domain-IB of HSA. Studies on binding of various drugs/ligands to different folded states of HSA are important as the conformation of carrier proteins depends on its immediate physiological environment. Moreover, clinical

* Corresponding author. Fax: +91 33 2335 3477.
E-mail address: skpal@bose.res.in (S.K. Pal).

1011-1344/$ - see front matter © 2007 Elsevier B.V. All rights reserved.
doi:10.1016/j.jphotobiol.2007.11.003

applications of HSA require good knowledge of thermal behavior of different folded states. Recently, advancement of time-resolved fluorescence and Fourier transform infrared spectroscopy for other proteins open a scope for direct observation of protein folding pathways [20–22]. Also, recent advancement in the field of nanosciences requires the preparation of bioactive nanoparticles under different temperature and pH conditions using protein molecules as templates [23–25]. Hence, search for a protein molecule, which can retain its overall structure under conditions widely differing from the physiological condition is highly demanding. It is known that HSA undergoes reversible conformational transformation with change in pH of the solution containing the protein [26,27]. At normal pH 7, HSA assumes the normal form (N) which abruptly changes to highly charged fast migrating form (F) at pH values less than 4.3, as this form moves "fast" upon gel electrophoresis [1]. Upon further reduction in pH to less than 2.7 the F-form changes to the fully extended form (E). On the basic side of the normal pH above pH 8, the N-form changes to basic form (B) and above pH 10, the structure changes to another aged form (A) [28]. Serum albumin undergoes an ageing process when stored at low ionic strength at alkaline pH. The ageing process is catalyzed by the free sulfhydryl group and involves sulfhydryl-disulfide interchange that results in the conservation of the sulfhydryl at its origin position. This A-form is stable and does not undergo N–F transition [28,29]. Several studies on thermal denaturation of serum albumins have been carried out using differential scanning calorimetric [30–34], electronic and vibrational circular dichroism [35] and fluorescence techniques [36]. Previous studies involving resonance energy transfer on pH-induced folded states of HSA has been done using steady-state fluorescence spectroscopy [37,38] and chemically denatured HSA using time-resolved fluorescence spectroscopy [36]. To our understanding till date there exist no energy transfer studies on the thermally induced conformers of HSA at different pH(s). In this report we have studied the conformational transformation of three pH-induced conformers of HSA at three different temperatures – 25, 60 and 75 °C using circular dichroism (CD) and dynamic light scattering (DLS) techniques. We have also measured the inter-domain separation between domain-I and domain-II applying Förster's resonance energy transfer (FRET) between Trp214 (donor) in domain-IIA and PPIX (acceptor) in domain-IB using picosecond time-resolved fluorescence techniques.

2. Materials and methods

Human serum albumin (HSA), protoporphyrin IX (PPIX), sodium acetate, sodium dihydrogen phosphate, disodium hydrogen phosphate were procured from sigma chemical (St. Louis, USA). Hydrochloric acid, sodium hydroxide and dimethyl formamide (DMF) were procured from Merck. Double distilled water was used for preparation of aqueous solutions. The molecular weight of HSA has been checked by MALDI mass spectrometry which essentially reveals a peak at 66.8 kDa (data not shown) consistent with the literature value [39]. All the other samples were used as received without further purification. Alkaline pH solutions were prepared by adding NaOH to phosphate buffer, while acidic pH solutions were prepared by adding HCl to acetate buffer. A stock solution of HSA was prepared in 10 mM phosphate buffer solution. HSA was labeled with PPIX as follows. About 3.5 mg of PPIX was dissolved in 100 μl DMF and injected in 5 aliquots of 20 μl each to 2 ml of phosphate buffer containing 200 μM HSA at an interval of 15 min under vigorous stirring condition. In order to prepare HSA–PPIX complex, the mixture was allowed to vigorously stir for 1 h and then a mild dialysis was carried out against phosphate buffer for 4.5 h to remove the unreacted PPIX. The HSA–PPIX solution was added in equal amounts to measured volumes of acidic/alkaline pH solutions and allowed to stir vigorously for two hours in order to achieve various pH-induced conformers of HSA–PPIX complexes. These samples were then used for spectroscopic studies.

Steady-state absorption and emission were measured with Shimadzu UV-2450 spectrophotometer and Jobin Yvon Fluoromax-3 fluorimeter respectively. The circular dichroism study was done using Jasco 815 spectropolarimeter using a quartz cell of path-length 10 mm. The secondary structural data of the CD spectra were analyzed using CDNN deconvolution program. Dynamic light scattering (DLS) measurements were done with Nano-S Malvern instruments (UK), employing a 4 mW He–Ne laser ($\lambda = 632.8$ nm) and equipped with a thermostatted sample chamber. All measurements were taken at 173° scattering angle at 298 K.

All the fluorescence transients were recorded using picosecond-resolved time correlated single photon counting (TCSPC) setup from Edinburgh instruments (LifeSpec-ps), UK. PPIX and Trp214 residue of HSA were excited using a laser source of 409 nm (Instrument response function, IRF ~ 86 ps) and a LED source of 299 nm (IRF ~ 460 ps), respectively. The observed fluorescence transients were fitted by using a nonlinear least square fitting procedure [40], the experimental details including the construction of temporal fluorescence anisotropy decay, $r(t)$ are published elsewhere [41].

In order to estimate the fluorescence resonance energy transfer efficiency of the donor Trp214 and hence to determine distances of donor–acceptor pairs, we followed the methodology described in chap. 13 of Ref. [42]. The Förster's distance (R_0) is given by,

$$R_0 = 0.211[\kappa^2 n^{-4} Q_D J(\lambda)]^{1/6} (\text{in Å}) \quad (1)$$

where κ^2 is a factor describing the relative orientation in space of the emission and absorption transition dipoles of the donor and acceptor, respectively. The value of the orientation factor κ^2 is calculated from the equation [42]

$$\kappa^2 = (\sin\theta_D \sin\theta_A \cos\phi - 2\cos\theta_D \cos\theta_A)^2 \quad (2)$$

where ϕ is the dihedral angle between the planes containing emission transition dipole of the donor and absorption transition dipole of the acceptor and θ_D and θ_A are the angles between these dipoles and the vector joining the donor and acceptor [42]. The refractive index (n) of the medium is assumed to be 1.4. Q_D, the quantum yield of the donor in the absence of acceptor is measured using the quantum yield of pure tryptophan (0.14) in buffer (pH 7) for Trp214 of HSA at different pH(s). $J(\lambda)$, the overlap integral, which expresses the degree of spectral overlap between the donor emission and the acceptor absorption is given by

$$J(\lambda) = \frac{\int_0^\infty F_D(\lambda)\varepsilon_A(\lambda)\lambda^4 \, d\lambda}{\int_0^\infty F_D(\lambda) \, d\lambda} \quad (3)$$

where $F_D(\lambda)$ is the fluorescence intensity of the donor in the wavelength range of λ to $\lambda + d\lambda$ and is dimensionless. $\varepsilon_A(\lambda)$ is the extinction coefficient (in $M^{-1}\,cm^{-1}$) of the acceptor at λ. If λ is in nm, then $J(\lambda)$ is in units of $M^{-1}\,cm^{-1}\,nm^4$. Once the value of R_0 is known, the donor–acceptor distance (R) can easily be calculated using the formula

$$R^6 = [R_0^6(1 - E)]/E \quad (4)$$

Here E is the efficiency of energy transfer. The transfer efficiency is measured using the average fluorescence lifetime, i.e., amplitude-weighted lifetimes ($\tau_{avg} = \Sigma\alpha_i\tau_i$) of the donor in the absence, τ_D and presence of acceptor, τ_{DA} as follows:

$$E = 1 - (\tau_{DA}/\tau_D) \quad (5)$$

The donor–acceptor (DA) distances (R) are measured using the above equations. The concentration of protein used for fluorescence measurement was about 7 μM in order to avoid intermolecular energy transfer between two protein molecules.

3. Results and discussions

The hydrodynamic diameters (d_H) of HSA at pH(s) 2, 7 and 11 are 14.3, 10.0 and 11.5 nm, respectively. It may indicate that the N-form HSA at pH 7 undergoes conformational transformation when pH is changed from 7 to 2, with subsequent acid-induced swelling/expansion of the HSA due to the disruption of domain structures (III and I) during N–E transition [43]. However, such structural change is not observed during N–A transition when pH is changed from 7 to 11. Another point to note from Fig. 1a is that N-form HSA (pH 7) does not show an increase in d_H value until 69 °C, thereafter d_H starts increasing sharply indicating cooperative temperature induced unfolding of HSA. The DLS spectra of N-form HSA at three different temperatures are shown in the insert of Fig. 1a. The d_H value at 75 °C is 19.9 nm. From the DLS spectra it can be observed that the overall size of N-form HSA remains same at 25 and 60 °C. However, at 75 °C the DLS spectrum is broad with peak at higher d_H value. In contrast to N-form HSA, the E-form (pH 2) and A-form (pH 11) HSA does not show any change in d_H values (Fig. 1a) with increase in temperature. The most plausible reason behind non-occurrence of thermal unfolding of E-form HSA is that this form has already assumed acid-induced expanded form [43] and also at pH ⩽4 gelification of HSA [32] takes place which further interferes with the thermal denaturation of the protein. In the alkaline pH range, the reason for no change in d_H value with temperature could be the increased stability of HSA due to high ionic strength of the alkaline solution [30].

Fig. 1b shows the CD spectra of N-form HSA at the above three temperatures. Comparison of the mean residual ellipticity of the three forms of HSA (figure not shown) at 25 °C shows that there is a significant loss of helix content for E-form HSA (see Table 1) due to disruption of inter-domain and intra-domain structure (domain- I and II) at pH 2 [43]. At pH 11 also, there is a decrease in helicity in comparison to native form (Table 1). It can be observed from Fig. 1b that with increase in temperature there is a gradual increase in molar ellipticity which indicates a loss of higher order secondary structure (α-helix) and increase in β-sheet and random structural content. This finding is consistent with the characteristics of HSA at higher temperature where the free –SH group at Cys34 exchanges with other disulfide bridges [30,32,36].

Fig. 2a shows the fluorescence spectra of N-form HSA at three different temperatures. It is found that with increase in temperature fluorescence peak (337 nm) exhibits 5 nm hypsochromic shift with reduction in fluorescence intensity. With increase in temperature, domain-II of HSA unfolds in such a way that Trp214 residue of HSA located at the bottom of 12 Å deep crevice [44] finds itself in a more hydrophobic environment [36]. Fluorescence peak data in Table 2 show that emission maximum at 337 nm for N-form shifts to 332 nm for E-form at pH 2 and that to 335 nm for A-form at pH 11. This is due the fact that at pH 2, although there occurs an increase inter-domain separation with disruption of the crevice containing Trp214, the local environment around Trp214 rearranges in such a way that the Trp finds itself in a more hydrophobic environment of the protein matrix [45]. Similarly, at pH 11, the minor changes in secondary structures causes it to be in hydrophobic environment. It is known that domain-II assumes a molten globule form at pH 2 [43]. Upon increasing the temperature to 75 °C the fluorescence maximum red shifts from 332 nm to 343 nm which may be due to the unfolding of domain-II below 60 °C followed by unfolding of domain-I above 60 °C causing Trp214 to come in contact with more polar environment (see Table 2). At pH 11, in contrast to pH 2, there occurs a slight blue shift of emission maximum with increase in temperature indicative of slightly hydrophobic environment around Trp214 at higher temperature. At all pH(s), there occurs a decrease in average fluorescence lifetime (τ_D) of Trp214, which may be due to the increased proximity with the quenching groups such as protonated carboxyl,

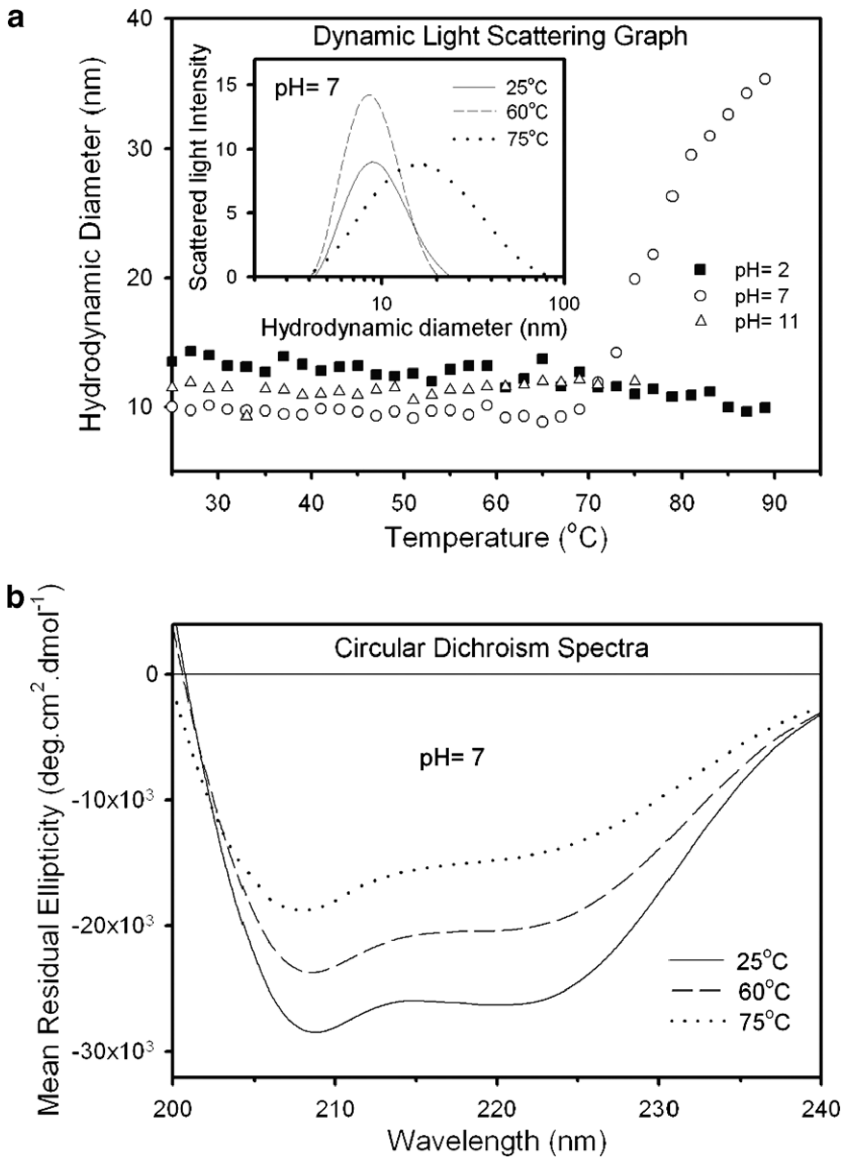

Fig. 1. (a) Graph of variation of hydrodynamic diameter of HSA versus temperature at pH 2, 7 and 11. Insert: Dynamic light scattering spectra of N-form HSA at 25, 60 and 75 °C. (b) Circular dichroism spectra of N-form HSA at 25, 60 and 75 °C.

Table 1
Percentages of secondary structures in different conformers of human serum albumin (HSA) at different temperatures

pH	Temperature (°C)	Secondary structures				
		Helix %	Antiparallel %	Parallel %	Turns %	Random %
2	25	59.5	4.3	4.5	13.2	18.5
	60	39.5	8.2	7.5	15.9	28.9
	75	31.9	8.2	9.3	16.9	33.7
7	25	66.2	3.3	3.3	12.2	15.0
	60	52.0	5.4	5.8	14.1	22.7
	75	38.0	8.0	8.1	16.0	29.9
11	25	60.4	3.9	4.0	13.0	18.7
	60	32.5	8.4	8.9	17.0	33.2
	75	15.5	12.5	12.3	19.4	40.3

protonated imidazole, deprotonated ε-amino groups, and tyrosinate anion [46,47] (see Table 2). At higher temperatures due to increased molecular dynamics and thus the increased frequency of collisions may also contribute to the lowering of average fluorescence lifetime. The emission spectra of PPIX labeled HSA at pH 7 and 11 are similar

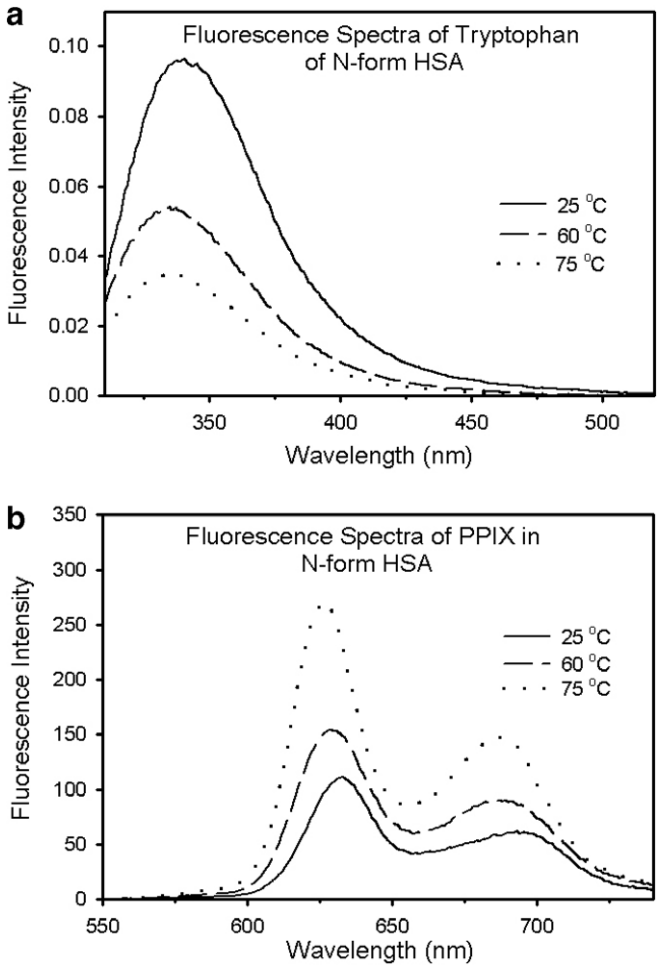

Fig. 2. (a) Fluorescence spectra of Tryptophan (Trp214) residue of N-form HSA (excitation = 297 nm) at 25, 60 and 75 °C, (b) fluorescence spectra of PPIX (excitation = 409 nm) bound to N-form HSA at 25, 60 and 75 °C.

with intense emission peak at 633 nm. However at pH 2, this band at 633 nm decreases in intensity with the appearance of two new peaks at 600 nm and 658 nm due to protonation [48] of intracyclic nitrogen atoms of PPIX. Fig. 2b shows the representative fluorescence spectra of PPIX bound to N-form HSA at different temperatures. Two peaks at ~630 nm and ~660 nm are observed which shows a gradual increase in fluorescence intensity with increasing temperature. However, for E-form HSA there is a gradual decrease while that for A-form HSA there is a decrease (at 60 °C) and then an increase (at 75 °C) of fluorescence intensity of PPIX. The longer fluorescence lifetime data of PPIX bound to HSA (Table 3) rules out the possibility of PPIX aggregation in presence of HSA [10]. The shorter lifetime of PPIX in HSA at acidic pH as evidenced from Table 3 could be due to the protonation of PPIX. Since both tryptophan [49] and PPIX [50] have multi-exponential fluorescence decays, their amplitude-weighted lifetime has been compared in our present work.

Fig. 3a–c shows the fluorescence anisotropy decay curve of PPIX bound to E, N and A conformers of HSA respectively at 25 and 75 °C. The data at 60 °C are not shown in Fig. 3 for the clarity of presentation. For all the conformations a longer rotational time constant of hundreds of nanoseconds consistent with the rotational correlation time (τ_{rot}) obtained from the Debye–Einstein–Stokes relation [51], $\tau_{rot}=4\pi\eta r3/3k_BT$ using the hydrodynamic diameter from DLS experiment, which does not decay in the experimental time window of 50 ns, is observed. This time corresponds to the global tumbling time of HSA conformers, which further indicates that at all conformations PPIX remains bound to the protein. A shorter rotational time constant of 0.2 ns is observed at pH 2 and 11 indicative of local reorientational motion of PPIX at its binding site. However, at pH 7 a faster time constant of 60 ps is observed indicating rapid librational motion of PPIX due to tighter binding of PPIX to native HSA. Fig. 4a shows the spectral overlap of emission spectra of the donor (Trp214 in domain-IIA) and the absorption spectrum of acceptor (PPIX in domain-IB) of N-form HSA. A significant overlap indicative of considerable non-radiative transfer of excited state energy from Trp214 to PPIX is observed. This is also evident from quenching of fluorescence of Trp214 as revealed from steady-state fluorescence spectra (Fig. 4b) and faster decay of Trp214 fluorescence (Fig. 4c) in presence of PPIX. The significant energy transfer and the large anisotropy of PPIX bound to HSA

Table 2
Calculated values of parameters obtained from FRET between Trp214 (domain-IIA) and PPIX (domain-IB) to different conformers of HSA at different temperatures

pH	Temperature (°C)	Peak (nm)	$<\tau_D>$ (ns)	$<\tau_{DA}>$ (ns)	$J(\lambda)$ M^{-1} cm^{-1} nm^4	E	R_0 (Å)	R (Å)
2	25	332	2.58	1.05	1.92×10^{15}	0.593	36.1	33.9
	60	334	0.99	0.50	1.87×10^{15}	0.495	30.7	30.8
	75	343	0.64	0.08	1.86×10^{15}	0.876	28.0	20.2
7	25	337	3.91	0.29	1.96×10^{15}	0.926	38.7	25.4
	60	332	1.96	0.03	1.69×10^{15}	0.984	33.9	17.0
	75	332	1.20	0.05	1.64×10^{15}	0.958	31.4	18.6
11	25	335	1.57	0.35	1.86×10^{15}	0.777	33.0	26.8
	60	331	0.38	0.11	1.75×10^{15}	0.697	33.1	28.8
	75	333	0.26	0.11	1.55×10^{15}	0.585	30.2	28.5

Table 3
Fluorescence maximum and average fluorescence lifetime (<τ>) of PPIX bound to different conformers of HSA at different temperatures

pH	Temperature (°C)	Wavelength (nm)	<τ> (ns)
2	25	604	6.62
	60	606	5.01
	75	608	4.14
7	25	633	9.74
	60	628	11.26
	75	626	12.64
11	25	625	13.98
	60	625	13.73
	75	626	13.39

provided the opportunity to apply Förster's resonance energy transfer theory in order to estimate the separation between PPIX and Trp214 and thus to determine the inter-domain separation. The average fluorescence lifetimes of Trp214 of HSA in presence and absence of PPIX are tabulated in Table 2. The calculated values of overlap integral ($J(\lambda)$), energy transfer efficiency (E), Förster's radius (R_0) and the donor–acceptor separation (R) are tabulated in Table 2 for different conformations of HSA.

The X-ray crystal structure of methemalbumin indicates that there is definite geometric arrangement of Haem605 and Trp214, thus κ^2 cannot be taken to be 0.67. In this case we have calculated the κ^2 value using Eq. (2) from the crystal structure of methemalbumin [19] and used the same for calculation of DA separation. The different angles were determined as follows. In the crystal structure [19] a straight line was drawn from the centre of Haem605 to the centre of indole moiety of Trp214 using WEBLAB VIEWERLITE software. Then the angles between this line and the molecular planes of Haem605 and Trp214 were measured to be 58.6° (θ_A) and 104.7° (θ_D). The dihedral angle (ϕ) between the molecular planes of Haem605 and Trp214 was measured to be 28.14°. The above measured angles gave a value of $\kappa^2 = 0.9853$. The DA separation of 25.4 Å obtained for N-form HSA at 25 °C is in close agreement with the distance (26.6 Å) between Trp214 and Haem605 obtained from X-ray crystallographic study of PPIX bound to HSA [19]. At pH 2 for E-form HSA, the DA separation of 33.9 Å is larger than that of N-form which is consistent with the increase in inter-domain separation and subsequent disruption of domain-I at 25 °C. Thus, significant loss of tertiary structure is observed at pH 2. Upon increasing the temperature, the separation decreases to 17.0 Å in N-form HSA indicating closer approach of Trp214 and PPIX. This may be due to disruption of domain-II of HSA due to which Trp214 becomes a bit flexible and moves closer to PPIX in domain-I. Again at 75 °C, a slight increase in DA separation to 18.6 Å may indicate the parting away of donor and acceptor due to disruption of domain-I above 60 °C. For E-form HSA at pH 2, however there is a decrease in DA separation from 25 °C till 75 °C. This may be due to the fact that in this acid-induced unfolded HSA where domain-II was in molten globule state starts unfolding with increase in temperature due to which DA separation decreases leading to proximity of donor and acceptor. Further increasing the temperature to 75 °C causes the conformation to change in such a way

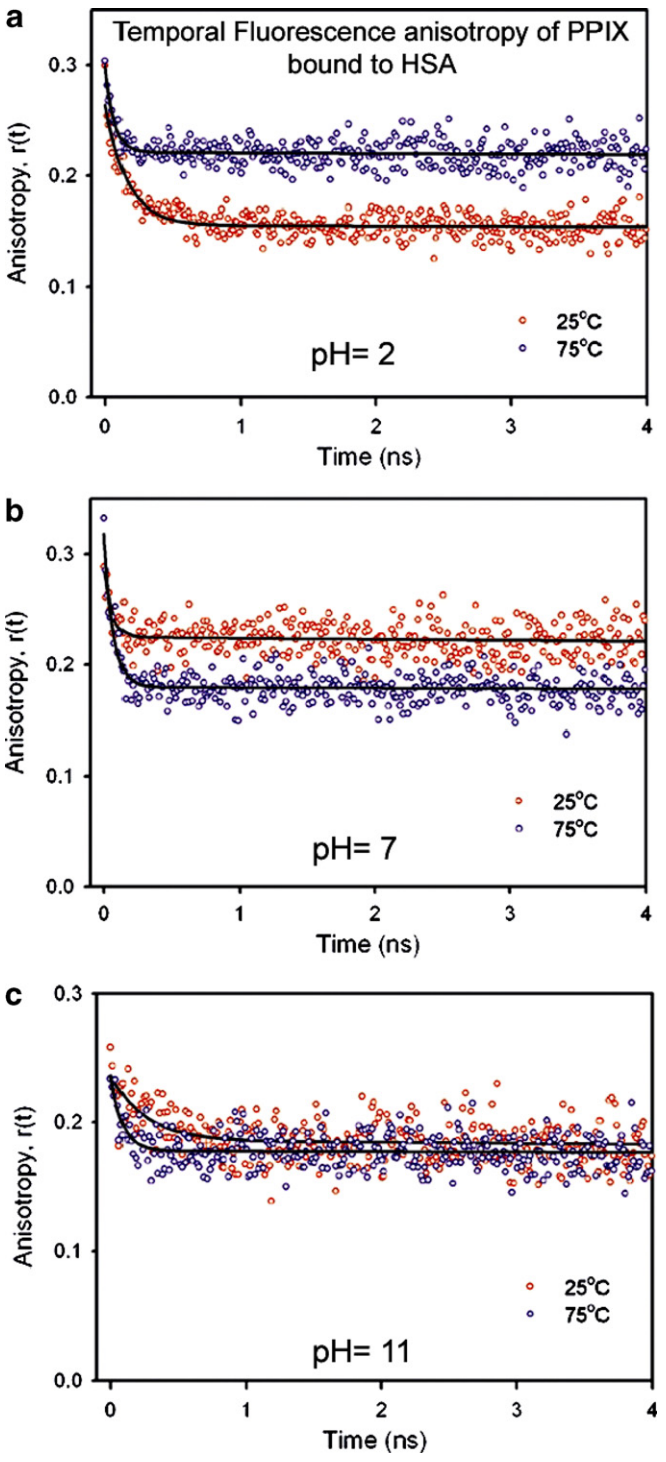

Fig. 3. (a) Temporal fluorescence anisotropy decay of PPIX bound to HSA (excitation = 409 nm) at pH(s): (a) 2 (emission = 605 nm), (b) 7 (emission = 630 nm) and (c) 11 (emission = 625 nm) at temperatures 25 and 75 °C.

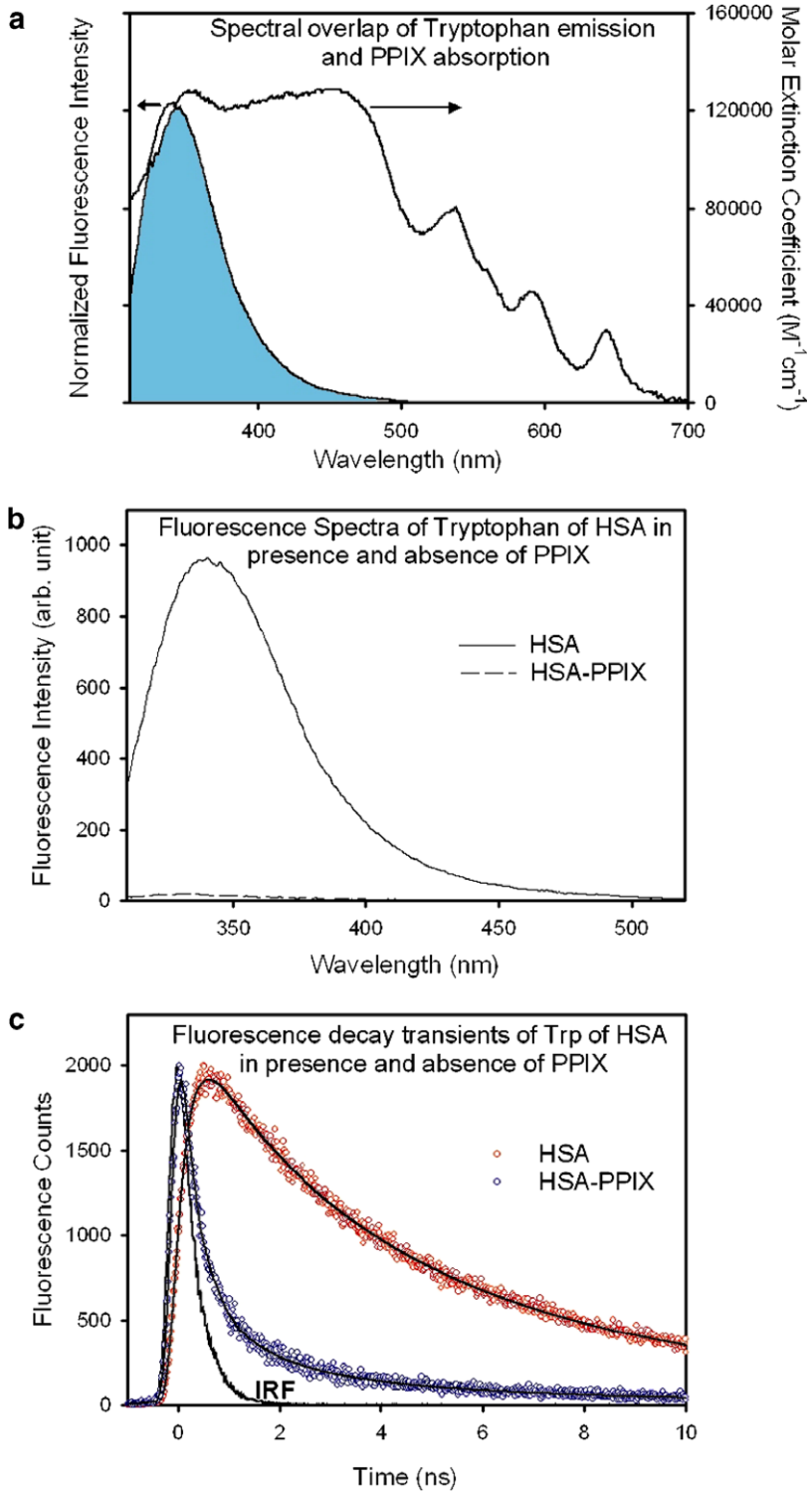

Fig. 4. (a) Spectral overlap of Fluorescence spectrum of Trp214 and absorption spectrum of PPIX bound to HSA at pH 7, (b) Fluorescence spectra (excitation = 297 nm) and (c) Fluorescence decay transients of Trp214 (excitation = 299 nm, emission = 360 nm) in presence and absence of PPIX bound to HSA at pH 7.

that there occurs a further reduction in DA separation. However, the A-form HSA at pH 11 shows almost no change in DA separation. This may be due to the fact that HSA attains greater stability in alkaline solution compared to neutral and acidic pH solutions.

4. Conclusion

In this study we have characterized the temperature induced unfolded states of an important multi-domain transporter protein, Human serum albumin (HSA). Using

steady state and time-resolved fluorescence spectroscopy we have characterized three different pH-induced conformers of HSA at three different temperatures. Applying Förster's resonance energy transfer (FRET) between the intrinsic donor fluorophore (Trp214) present in domain-IIA and a photosensitizer protoporphyrin IX (PPIX) (acceptor) bound to domain-IB of HSA, we have determined the distance between the donor and acceptor in the different temperature-induced folded conformers of HSA. CD studies carried out for different conformers at various pH(s) indicate significant loss of secondary structures in comparison to the native HSA at neutral pH. DLS studies show that although there occurs a significant temperature induced unfolding for N-form HSA, no such unfolding is observed for the other acid and alkali-induced conformers. From the FRET study, it is observed that with increase in temperature the distance between donor and acceptor decreases for E and N conformers of HSA while that for A conformer the distance remains unchanged which is consistent with the salt stabilized HSA at higher ionic strength in alkaline solution. Finally, this study on different conformations of HSA at different temperatures reflects the efficiency of a non-covalently bound probe, PPIX to act as an acceptor for applying FRET technique.

Acknowledgement

AKS thanks UGC for fellowship. We thank DST for financial grant (SR/FTP/PS-05/2004).

References

[1] J.F. Foster, Some aspects of the structure and conformational properties of serum albumin, in: V.M. Rosenoer, M. Oratz, M.A. Rothschild (Eds.), Albumin, Structure, Function and Uses, Pergamon, Oxford, 1977.
[2] B. Honore, A.O. Pedersen, Conformational changes in human serum albumin studied by fluorescence and absorption spectroscopy. Distance measurements as a function of pH and fatty acids, Biochem. J. 58 (1989) 199–204.
[3] T.J. Peters, All about Albumin: Biochemistry, Genetics and Medical Applications, Academic Press, Orlando, FL, 1996.
[4] X.M. He, D.C. Carter, Atomic structure and chemistry of human serum albumin, Nature 358 (1992) 209–215.
[5] J. Ghuman, P.A. Zunszain, I. Petitpas, A.A. Bhattacharya, M. Otagiri, S. Curry, Structural basis of the drug-binding specificity of human serum albumin, J. Mol. Biol. 353 (2005) 38–52.
[6] C.M. Dobson, The structural basis of protein folding and its links with human disease, Philos. Trans. R. Soc. B 356 (2001) 133–145.
[7] V. Jain, H. Goel, in: V. Jain (Ed.), Selected Topics in Photobiology, Indian Photobiological Society, New Delhi, 1992, pp. 130–147.
[8] A.M. Joussen, F.E. Kruse, M. Kaus, H.E. Volcker, Endogenous porphyrin for photodynamic therapy of cataracts in vitro, Opthalmologe 94 (1997) 428–435.
[9] J.M. Nauta, O.C. Speelman, H.L. van Leengoed, P.G. Nikkels, J.L. Roodenburg, W.M. Star, M.J. Witjes, A.J. Vermey, In vivo photodetection of chemically induced premalignancy lesions and squamous cell carcinoma of the rat palatal mucosa, Photochem. Photobiol. B: Biol. 39 (1997) 156–166.
[10] N.C. Maiti, S. Mazumdar, N. Periasamy, Dynamics of porphyrin molecules in micelles. Picosecond time-resolved fluorescence anisotropy studies, J. Phys. Chem. 99 (1995) 10708–10715.
[11] N.C. Maiti, M. Ravikanth, S. Mazumdar, N. Periasamy, Fluorescence dynamics of noncovalently linked porphyrin dimers and aggregates, J. Phys. Chem. 99 (1995) 17192–17197.
[12] N.C. Maiti, S. Mazumdar, N. Periasamy, J- and H-Aggregates of porphyrin–surfactant complexes: time-resolved fluorescence and other spectroscopic studies, J. Phys. Chem. B 102 (1998) 1528–1538.
[13] M.Y. Okamura, G. Feher, D.L. Nelson, in: Govindjee (Ed.), Photosynthesis, Academic Press, 1982, pp. 195–272.
[14] P. Kubat, K. Lang, P. Anzenbacher Jr., Modulation of porphyrin binding to serum albumin by pH, Biochim. Biophys. Acta 1670 (2004) 40–48.
[15] S.M. Andrade, S.M.B. Costa, Spectroscopic studies on the interaction of a water soluble porphyrin and two drug carrier proteins, Biophys. J. 82 (2002) 1607–1619.
[16] Y.-B. Yin, Y.-N. Wang, J.-B. Ma, Aggregation of two carboxylic derivatives of porphyrin and their affinity to bovine serum albumin, Spectrochim. Act A 64 (2006) 1032–1038.
[17] R. Galantai, I. Bardos-Nagy, K. Modos, J. Kardos, P. Zavodszky, J. Fidy, Serum albumin–lipid membrane interaction influencing the uptake of porphyrins, Arch. Biochem. Biophys. 373 (2000) 261–270.
[18] S. Cohen, R. Margalit, Binding of porphyrin to human serum albumin: structure–activity relationships, Biochem. J. 270 (1990) 325–330.
[19] M. Wardell, Z. Wang, J.X. Ho, J. Robert, F. Ruker, J. Ruble, D.C. Carter, The atomic structure of human methemalbumin at 1.9 Å, Biochem. Biophys. Res. Comm. 291 (2002) 813–819.
[20] R. Sarkar, A.K. Shaw, S.S. Narayanan, F. Dias, A. Monkman, S.K. Pal, Direct observation of protein folding in nanoenvironments using a molecular ruler, Biophys. Chem. 123 (2006) 40–48.
[21] C. Kotting, K. Gerwert, Time-resolved FTIR studies provide activation free energy, activation enthalpy and activation entropy for GTPase reactions, Chem. Phys. Lett. 307 (2004) 227–232.
[22] C. Kotting, K. Gerwert, Proteins in action monitored by time-resolved FTIR spectroscopy, ChemPhysChem 6 (2005) 881–888.
[23] J.-G. Liang, X.-P. Ai, Z.-K. He, H.-Y. Xie, D.-W. Pang, Synthesis and characterization of CdS/BSA nanocomposites, Mater. Lett. 59 (2005) 2778–2781.
[24] R. Sarkar, S. Shankara Narayanan, L.-O. Pa°lsson, F. Dias, A. Monkman, S.K. Pal, Direct conjugation of semiconductor nanocrystals to a globular protein to study protein-folding intermediates, J. Phys. Chem. B 111 (2007) 12294–12298.
[25] S. Shankara Narayanan, R. Sarkar, S.K. Pal, Structural and functional characterization of enzyme-quantum dot conjugates: covalent attachment of CdS nanocrystal to r-chymotrypsin, J. Phys. Chem. C 111 (2007) 11539–11543.
[26] J.A. Luetscher, Serum albumin. II. Identification of more than one albumin in horse and human serum by electrophoretic mobility in acid solution, J. Am. Chem. Soc. 61 (1939) 2888–2890.
[27] J.F. Foster, The Plasma Proteins, Academic Press, New York, 1960.
[28] H.J. Nikkel, J.F. Foster, A reversible sulfhydryl-catalyzed structural alteration of bovine mercaptalbumin, Biochemistry 10 (1971) 4479–4486.
[29] C.N. Cornell, L.J. Kaplan, Spin-label studies of the sulfhydryl environment in bovine plasma albumin. 2. The neutral transition and the A isomer, Biochemistry 17 (1978) 1755–1758.
[30] M. Yamasaki, H. Yano, K. Aoki, Differential scanning calorimetric studies on bovine serum albumin: I. Effects of PH and ionic strength, Int. J. Biol. Macromol. 12 (1990) 263–268.
[31] C. Giancola, C.D. Sena, D. Fessas, G. Graziano, G. Barone, DSC studies on bovine serum albumin denaturation. Effects of ionic strength and SDS concentration, Int. J. Biol. Macromol. 20 (1997) 193–204.
[32] G. Barone, C. Giancola, A. Verdilova, DSC studies on the denaturation and aggregation of serum albumins, Thermochim. Acta 199 (1992) 197–205.

[33] B. Farruggia, G.A. Pico, Thermodynamics features of the chemical and thermal denaturations of human serum albumin, Int. J. Biol. Macromol. 26 (1999) 317–323.
[34] G.A. Pico, Thermodynamic features of the thermal unholding of human serum albumin, Int. J. Biol. Macromol. 20 (1997) 63–73.
[35] G. Shanmugam, P.L. Polavarapu, Vibrational circular dichroism spectra of protein films: thermal denaturation of bovine serum albumin, Biophys. Chem. 111 (2004) 73–77.
[36] K. Flora, J.D. Brennan, G.A. Baker, M.A. Doody, F.V. Bright, Unfolding of acrylodan-labeled human serum albumin probed by steady-state and time-resolved fluorescence methods, Biophys. J. 75 (1998) 1084–1096.
[37] N. Hagag, E.R. Birnbaum, D.W. Darnall, Resonance energy transfer between cysteine-34, tryptophan-214, and tyrosine-411 of human serum albumin, Biochemistry 22 (1983) 2420–2427.
[38] M. Suzukida, H.P. Le, F. Shahid, R.A. Mcpherson, E.R. Birnbaum, D.W. Darnall, Resonance energy transfer between cysteine-34 and tryptophan-214 in human serum albumin. Distance measurements as a function of pH, Biochemistry 22 (1983) 2415–2420.
[39] M. Dockal, D.C. Carter, F. Ruker, The three recombinant domains of human serum albumin, J. Biol. Chem. 274 (1999) 29303–29310.
[40] D.V. O'Connor, D. Philips, Time Correlated Single Photon Counting, Academic Press, London, 1984.
[41] A.K. Shaw, S.K. Pal, Fluorescence relaxation dynamics of acridine orange in nanosized micellar systems and DNA, J. Phys. Chem. B 111 (2007) 4189–4199.
[42] J.R. Lakowicz, Principles of Fluorescence Spectroscopy, Kluwer Academic/Plenum, New York, 1999.
[43] M. Dockal, D.C. Carter, F. Ruker, Conformational transitions of the three recombinant domains of human serum albumin depending on pH, J. Biol. Chem. 275 (2000) 3042–3050.
[44] W. Qiu, L. Zhang, O. Okobiah, Y. Yang, L. Wang, D. Zhong, A.H. Zewail, Ultrafast solvation dynamics of human serum albumin: correlations with conformational transitions and site-selected recognition, J. Phys. Chem. B 110 (2006) 10540–10549.
[45] M.R. Eftink, C.A. Ghiron, Exposure of tryptophyl residues in proteins. Quantitative determination by fluorescence quenching studies, Biochemistry 15 (1976) 672–679.
[46] C.J. Halfman, T. Nishida, Influence of pH and electrolyte on the fluorescence of bovine serum albumin, Biochim. Biophys. Acta 243 (1971) 284–293.
[47] C.J. Halfman, T. Nishida, Nature of the alteration of the fluorescence spectrum of bovine serum albumin produced by the binding of dodecyl sulfate, Biochim. Biophys. Acta 243 (1971) 294–303.
[48] R.C. Srivastava, V.D. Anand, W.R. Carper, A fluorescence study of hematoporphyrin, Appl. Spectrosc. 27 (1973) 444–449.
[49] X.H. Shen, J. Knutson, Subpicosecond fluorescence spectra of tryptophan in water, J. Phys. Chem. B 105 (2001) 6260–6265.
[50] L. Brancaleon, S.W. Magennis, I.D.W. Samuelb, E. Namdasb, A. Lesara, H. Moseleya, Characterization of the photoproducts of protoporphyrin IX bound to human serum albumin and immunoglobulin G, Biophys. Chem. 109 (2004) 351–360.
[51] P. Debye, Polar Molecules, Dover, New York, 1929.